Diffusion-induced growth of GaAs nanowhiskers during molecular beam epitaxy: Theory and experiment

V. G. Dubrovskii,[1,*] G. E. Cirlin,[1,2] I. P. Soshnikov,[1] A. A. Tonkikh,[1,2] N. V. Sibirev,[2] Yu. B. Samsonenko,[1,2] and V. M. Ustinov[1]

[1]*Ioffe Physical Technical Institute of the Russian Academy of Sciences, Politekhnicheskaya 26, 194021, St.-Petersburg, Russia*

[2]*Institute for Analytical Instrumentation of the Russian Academy of Sciences, Rizhsky 26, 190103, St.-Petersburg, Russia*

(Received 25 October 2004; revised manuscript received 12 January 2005; published 31 May 2005)

Mechanisms of nanowhisker formation during molecular beam epitaxy (MBE) are studied theoretically within the frame of a kinetic model that accounts for the adatom diffusion from the surface to the top of nanowhiskers. It is shown that the adatom diffusion flux may considerably increase the vertical growth rate of nanowhiskers. The decreasing length/diameter dependence of the MBE grown nanowhiskers is obtained that explains a number of experimentally observed facts. The results of experimental investigations of GaAs nanowhiskers grown by MBE on the GaAs(111)B surface activated by Au at different conditions are presented and analyzed. It is shown that the length of thin GaAs nanowhiskers is several times larger than the effective thickness of deposited GaAs. Theoretical and experimental length/diameter curves are compared to each other and a good correlation between them is demonstrated.

DOI: 10.1103/PhysRevB.71.205325 PACS number(s): 68.65.−k, 68.47.Fg, 68.70.+w, 81.10.Aj

I. INTRODUCTION

Nanowhiskers, or vertical nanowires (NWs), are wirelike nanocrystals with the diameter of several tens of nm and the length/diameter ratios of 10 and more.[1] NWs are one-dimensional objects with unique structural and electronic properties and therefore attract an increasingly growing interest towards their applications in novel microelectronic and optoelectronic devices.[2–4] Semiconductor NWs (Si, GaAs) are usually grown by chemical vapor deposition (CVD) (Refs. 5–8 and 10) or molecular beam epitaxy (MBE) (Refs. 9 and 10) on the surfaces activated by a growth catalyst. One of the first examples of catalytic growth of whiskers was demonstrated by Wagner and Ellis[11] in their experiments with the CVD growth of Si on the Si(111) surface activated by Au. One of the critical issues in the physics of NWs and in their utilization in devices is the understanding of NW formation mechanisms. This is important for the development of reliable nanofabrication techniques with controllably structured NWs for different applications. Also, the growth behavior of NWs is interesting from the viewpoint of fundamental physics as a very rare example of one-dimensional catalytic growth of nanocrystals.

Typical procedure of NW formation is the following.[1] First, the catalyst (e.g., Au) is deposited onto a crystal substrate (e.g., GaAs) and annealed before the whiskers are grown. Annealing leads to the formation of droplets of eutectic liquid alloy (e.g., Au-GaAs) on the substrate surface. The deposition of semiconductor material (GaAs) from the vapor phase or molecular beam leads to the epitaxial growth on the surface. The key effect of activation is that the surface under the drops grows much faster than the surface without catalyst. The usual explanation of this effect is the so-called vapor-liquid-solid (VLS) mechanism of whisker growth,[11] which has been subsequently extended to include the nanometer scale and is now widely used for the explanation of NW formation.[12] In VLS mechanism, whiskers are assumed to grow due to the adsorption of vapor atoms on the drop surface and their transfer to the crystal phase due to the solidification of liquid alloy on the crystal surface under the drop. The higher growth rate of whiskers in the VLS mechanism is explained by a faster chemical reaction or better adsorption on the liquid surface and a faster nucleation of crystal phase from the liquid drop. Since the initial eutectic drops usually have a broad size distribution and the whisker lateral size is usually of order of the size of drop, the lateral size dependence of the normal growth rate of whiskers has been studied experimentally in many systems.[12–14] It has been found that in VLS growth whisker length L normally increases with their diameter D; thicker whiskers thus grow faster than thinner ones. For very thick whiskers the growth rate is determined by the balance of adsorption and desorption processes on the planar surface of liquid alloy. Givargizov[15] suggested to attribute the observed increase of $L(D)$ curves to the Gibbs-Thomson effect caused by the finite curvature of the whisker surface. The Givargizov-Chernov theory[15,16] provides for the whisker growth rate dL/dt the expression of the form $dL/dt=(A-B/D)^2$. The coefficients A and B depend on the CVD growth conditions and the vapor-solid interfacial energy. This theory also explains the existence of a certain minimum diameter of drop under which the whiskers would not grow. Recently some of the authors of this paper proposed a more detailed kinetic model of VLS growth of NWs.[17] In particular, it has been shown that under certain assumptions the NW growth rate can be indeed approximated by a quadratic function of $1/D$ and that dL/dt in this case is inversely proportional to the squared interfacial energy of liquid-surface boundary. This explains a higher rate of layer-by-layer growth of crystal under the drop. However, the model of Ref. 17 also gives an increasing $L(D)$ dependence and the maximum growth rate of NWs is limited by the deposition rate of the material.

At the moment, semiconductor NWs are mainly grown by CVD.[1,5–7] However, MBE technique provides a number of

advantages in the NW technology[9,14] due to strongly nonequilibrium conditions during the MBE growth at lower substrate temperatures.[18] Since MBE growth always proceeds at higher supersaturations of gaseous phase, it may provide an opportunity to achieve larger L/D ratios at smaller diameters D. However, the mechanisms of NW formation during MBE remain in largest measure unformulated. In contrast to the majority of CVD techniques of NW formation, in MBE growth the nonactivated surface may grow with the rate comparable to the deposition rate. Here the question arises: if the maximum growth rate of NWs is limited by the deposition rate, why is their length much higher than the nominal thickness of deposited material? In contrast to CVD, the MBE growth implies very high values of the diffusion length of adsorbed atoms (adatoms) $\sim 1-10$ μm, which is of order or higher than the typical whisker lengths. Therefore, the contribution of the adatom diffusion into the overall growth behavior of NWs should be carefully investigated. An important step in studying the mechanisms of NW formation during MBE was taken by Schubert *et al.*,[19] who reported the $L(D)$ dependence of Si whiskers grown on the Si(111)-Au surface. Expecting the usual VLS growth to proceed, the authors found that narrower whiskers grew much faster than the thicker ones. The measured $L(D)$ dependence was found to be close to the inversely proportional relation $L \propto A/D$. Such form of $L(D)$ dependence is typical for the diffusion-induced (DI) growth of wirelike crystals that was investigated theoretically and experimentally by Sears[20,21] and Dittmar and Neumann.[22,23] DI growth is controlled by the diffusion of adatoms towards the whisker top along their side facets. When the surface is activated by the growth catalyst, the drop of a liquid alloy on the top of NW may be quite an attractor for the adatoms and VLS growth may take many features of the DI one. Technologically it is important that MBE technique may enable growing whiskers whose length is much higher than the effective thickness of deposited material (when the DI mechanism dominates), because the growth rate of NWs in the DI mode is no longer restricted by the deposition rate.

The aim of this work is theoretical and experimental investigation of NW formation mechanisms during MBE. A kinetic model of NW formation will be presented that handles the description of adatom diffusion from the surface of epitaxially growing layer to the NW tops. Experimental results on the MBE growth of GaAs NWs on the GaAs(111)B surface activated by Au will be reported and compared to the predictions of the theoretical model. It will be demonstrated experimentally that under certain conditions MBE method enables one to realize pure DI growth mode and to grow whiskers with lengths much higher than the effective thickness of deposited GaAs. A theoretical model will explain why such a growth behavior of NWs may occur.

II. THEORETICAL MODEL

Thermodynamic driving force for the formation of NWs on an activated surface is the difference of chemical potentials in the gaseous, liquid, and solid phases. The adsorption on the drop surface dominates over desorption only when the supersaturation in the gaseous phase is higher than the supersaturation of the liquid alloy. The crystallization of liquid on the solid surface under the drop is possible only when the alloy is supersaturated. The VLS growth of NWs strongly depends on the phase diagram of catalyst and deposited material, the values of interfacial energies on gas-liquid, liquid-solid, and gas-solid boundaries. The corresponding expressions can be found, for example, in Ref. 17. In this work we try to incorporate the DI effects into the standard VLS concept; therefore we consider the model of NW growth during MBE on activated surface as shown schematically in Fig. 1. In this model the normal growth of NWs is ensured by the crystallization of the material from the supersaturated liquid alloy in the drop on the crystal surface under the drop (as in VLS growth). However, we assume that the atoms may arrive into the drop not only from the molecular beam but also from the substrate surface due to diffusion along the side facets of NWs (as in DI growth). Obviously, the diffusion motion from the surface to the drop is possible only when the adatom supersaturation on the surface σ is higher than the supersaturation of liquid alloy ζ. In steady state the normal growth rate of NW dL/dt is given by

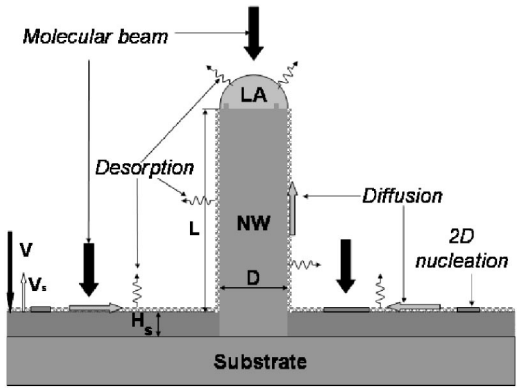

FIG. 1. The model of NW growth during MBE. NW is assumed as being a cylinder of diameter $D=2R$ and length L, the contact angle of drop is assumed to be 90°. The processes on the main surface are adsorption, desorption, diffusion, and nucleation; the processes on the side surface of NW are desorption and diffusion; the processes on the NW top are adsorption and desorption on the liquid surface and the vertical growth of the top facet. The deposition rate from a molecular beam is V, the surface growth rate is V_s, and the NW growth rate is dL/dt.

$$\frac{\pi R^2}{\Omega}\frac{dL}{dt} = \left(\frac{V - V_s}{\Omega} - \frac{2Cr_l}{\tau_l}\right)\pi R^2 + j_L. \tag{1}$$

Here $L(t)$ is the NW length at time t measured from the surface of the epitaxial layer, growing on the substrate surface and having the thickness of $H_s(t)$ (Fig. 1), R is the NW radius, V_s is the growth rate of nonactivated surface, V is the deposition rate, Ω is the volume per atom in the crystal, C is the volume concentration of alloy, r_l is the interatomic distance in the liquid phase, τ_l is the mean lifetime of atoms in the liquid, and j_L is the diffusion flux of adatoms towards the top of NW. The first term in Eq. (1) stands for adsorption on the liquid surface, the second for the desorption, and the

third describes the DI contribution to the growth rate. Below we consider the growth rate of nonactivated surface V_s as being the model parameter that can be obtained from the experimentally recorded data.[19] Since the diffusion length of adatoms on the surface is much larger than R [in the case of GaAs(111)B surface at 580 °C, the diffusion length of Ga atoms is several μm (Ref. 24)], we can assume σ near the NW base as being coordinate independent. In a simplified model we will consider σ as the second model parameter. Generally the parameters V_s and σ are related to each other and are the functions of the lateral size distribution of NWs. When the 2D nucleation on the side surface of NW is not pronounced (no lateral growth of NW), the adatom concentration on the side surface changes due to (i) desorption and (ii) surface diffusion. In contrast to CVD, in MBE there is no adsorption on the side surface of vertically standing whiskers. Therefore, in steady state the kinetic equation for adatom supersaturation on the side surface η reads

$$-(\eta+1)\frac{1}{\tau_f}+D_f\frac{\partial^2}{\partial z^2}\eta=0. \tag{2}$$

Here z is the coordinate along the whisker axis, D_f is the diffusion coefficient of the adatom on the side surface of NW, and τ_f is the lifetime of the adatom on the side surface before reevaporation. The first boundary condition to Eq. (2) is found from the equation of continuity at $z=0$

$$j_0 = -D_f n_{\mathrm{eq}} 2\pi R\frac{d\eta}{dz}\bigg|_{z=0}=\frac{l_s}{4t_s}2\pi R N_{\mathrm{eq}}\sigma. \tag{3}$$

Equation (3) indicates that the adatom flux through the NW base j_0 equals the number of adatoms attached to the NW boundary. Here n_{eq} is the equilibrium concentration of adatoms on the side surface, N_{eq} is the equilibrium concentration of adatoms on the main surface, l_s is the length of adatom diffusion jump on the main surface, and t_s is the characteristic time between two consecutive diffusion jumps. The attachment rate is proportional to adatom supersaturation σ,[25] The second boundary condition to Eq. (2)

$$\eta(z=L)=\zeta \tag{4}$$

means that the adatom supersaturation goes to the supersaturation of the liquid alloy at $z=L$. Solution to Eq. (2) with boundary conditions (3) and (4) enables one to find $\eta(z)$ and therefore to calculate the adatom diffusion flux to the NW top

$$j_L = -D_f n_{\mathrm{eq}} 2\pi R\frac{d\eta}{dz}\bigg|_{z=L}. \tag{5}$$

The result for j_L is obtained from Eqs. (2)–(5) in the form

$$j_L=\beta\left[\frac{\alpha\sigma}{\cosh(\lambda)}-\tanh(\lambda)(\zeta+1)\right]. \tag{6}$$

Here $\lambda\equiv L/L_f$ is the ratio of whisker length to the adatom diffusion length on the side surface $L_f=\sqrt{D_f\tau_f}$. Coefficients α and β are determined by the physical parameters of the system and by the radius of NW R as follows:

$$\alpha\equiv\frac{l_s L_f}{4t_s D_f}\frac{N_{\mathrm{eq}}}{n_{\mathrm{eq}}},\quad \beta\equiv\frac{D_f n_{\mathrm{eq}}}{L_f}2\pi R. \tag{7}$$

Estimating the diffusion coefficient as $D_f=l_f^2/t_f$, where l_f is the length of diffusion jump on the side surface and t_f is the corresponding diffusion time, at $N_{\mathrm{eq}}\sim n_{\mathrm{eq}}$, $t_f\sim t_s$, and $l_f\sim l_s$ we get $\alpha\sim L_f/4l_f\sim 10^3$, because the diffusion length of Ga on the GaAs(110) surface at 580 °C is of order of 10 μm (Ref. 26) and the length of diffusion jump is of order of lattice spacing. The adatom supersaturation on the surface is normally of order of unity[25] and the supersaturation of liquid alloy is very small.[13] Also, the length of the longest NWs is normally not higher than 10 μm. Therefore, at $\lambda\ll 1$ and $\lambda\sim 1$ the first term on the right-hand side of Eq. (6) dominates and the term containing $\zeta+1$ can be neglected. Under the same assumptions the concentration of alloy C in Eq. (1) can be put to its equilibrium value C_{eq}. The approximate expression for the NW growth rate is therefore reduced to

$$\frac{dL}{dt}=V\left[\varepsilon-\gamma+\frac{R_c}{R\cosh(\lambda)}\right]. \tag{8}$$

The coefficient γ accounts for the desorption from the drop surface:

$$\gamma\equiv\frac{2C_{\mathrm{eq}}r_l\Omega}{V\tau_l}\cong\frac{2x_{\mathrm{eq}}}{W\tau_l}, \tag{9}$$

where x_{eq} is the equilibrium percent concentration of the liquid alloy and W is the deposition rate in monolayers per second (ML/s). The coefficient $\varepsilon\equiv(V-V_s)/V$ is the relative difference between the deposition rate V and surface growth rate V_s. The radius R_c gives the characteristic scale at which the DI effects become predominant:

$$R_c\equiv\frac{\Omega l_s N_{\mathrm{eq}}}{2Vt_s}\sigma=\frac{\theta_{\mathrm{eq}}l_s}{Wt_s}\sigma, \tag{10}$$

where θ_{eq} is the equilibrium adatom coverage of the surface.

Taking for estimates the typical numbers[13,25] $x_{\mathrm{eq}}\sim 0.1$, $W\sim 1$ ML/s, $\tau_l\sim 1$ s, $\theta_{\mathrm{eq}}\sim 5\times 10^{-3}$, $l_s\sim 0.4$ nm, $t_s\sim 10^{-5}$ s, and $\sigma\sim 1$ we get $\gamma\sim 0.2$ and $R_c\sim 100$ nm. Therefore, desorption from the liquid drop may reduce the vertical growth rate of NW up to 20%. However, for thin NWs with $R\sim 10$ nm the adatom diffusion may increase the growth rate in order of magnitude. All DI contributions die at $R\to\infty$ as $1/R$, because the adatom flux to the whisker top is proportional to R and the adsorption-desorption term is proportional to R^2. Equation (8) also shows that the DI contribution vanishes at $\lambda\to\infty$, because all adatoms reevaporate before they reach the NW top. Solution to Eq. (8) can be presented in the form

$$L(t)=V(\varepsilon-\gamma)t+L_f I(\varphi,\lambda). \tag{11}$$

The first term in the right-hand side of Eq. (11) equals the adsorption-desorption VLS growth rate $(1-\gamma)V$ minus the surface growth rate $V_s=(1-\varepsilon)V$; this term can be of either signs. The DI contribution contains the function I of the form

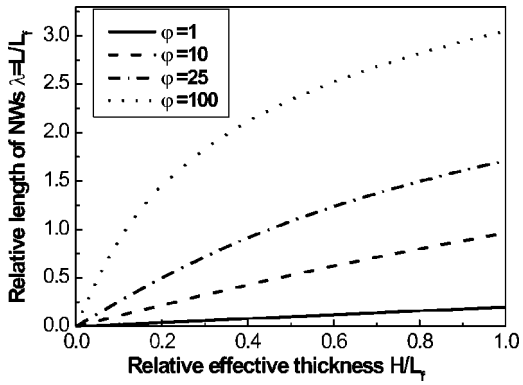

FIG. 2. Dependences of relative length of NWs L/L_f on the relative effective thickness of deposited material H/L_f at different drop diameters $[\varphi \equiv R_c/R(\varepsilon-\gamma_l)]$ obtained from Eqs. (12) and (13).

$$I(\varphi,\lambda) = \varphi \int_0^{\lambda} \frac{dx}{\varphi + \cosh(x)} \tag{12}$$

with $\varphi \equiv R_c/R(\varepsilon-\gamma)$. At $\varphi \gg 1$ (thin NWs with $R \ll R_c$ at arbitrary ε and γ or $\varepsilon-\gamma \ll 1$ relating to the case when very thick whiskers grow with the same rate as the surface), solutions (11) and (12) are reduced to

$$\sinh(\lambda) = \left(\frac{R_c}{R} + \varepsilon - \gamma\right)\frac{Vt}{L_f}. \tag{13}$$

For relatively short NWs with $\lambda \ll 1$ Eq. (13) is further simplified to

$$L = \frac{R_c}{R} Vt. \tag{14}$$

The NW length in this case is inversely proportional to the NW diameter. This dependence was observed experimentally for the Si NWs grown by MBE on the Si(111)-Au surface.[19]

Typical growth kinetics of NWs in the DI mode is shown in Figs. 2 and 3. As seen from Fig. 2, for modest values of effective thickness H, the NW length linearly depends on H; for larger H this dependence converts to logarithmical. Figure 3 demonstrates that at given H the length of NWs

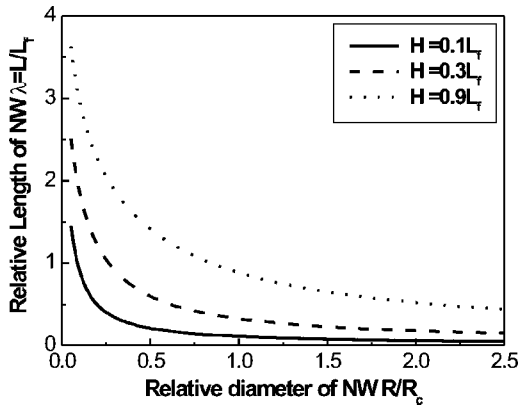

FIG. 3. Dependences of NW length L/L_f on their diameter R/R_c obtained from Eqs. (12) and (13) at three different values of the effective thickness of deposited material H/L_f, $\varepsilon=0.3$, and $\gamma=0.2$.

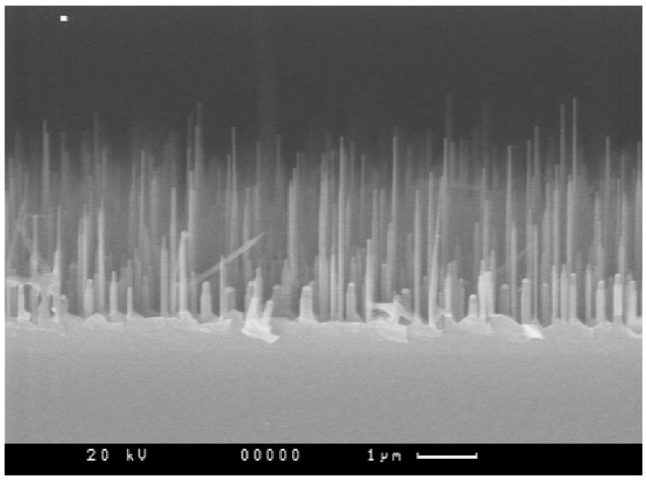

FIG. 4. SEM image of sample 1, $d_{Au}=1.0$ nm, effective thickness of GaAs=500 nm.

strongly increases at smaller drop diameters, which is typical for the DI growth.[20–23]

III. EXPERIMENT

In our growth experiments, the NW formation procedure consisted of three stages.[14] First, GaAs(111)B substrates were placed in the growth chamber of the EP1203 MBE setup, where the oxide was removed from the substrates and the GaAs buffer layer was deposited. The GaAs buffer layer thickness was kept about 300 nm in all growth runs. Second, the samples were transferred from the MBE setup into the vacuum chamber equipped with an Au electron beam evaporator. In the vacuum chamber, a thin Au film was deposited onto the sample surface. The Au film thickness d_{Au} amounted to 1.0 nm (sample No. 1) and 2.5 nm (sample No. 2). Third, the samples were transferred back to the MBE growth chamber, heated up to the temperature of 630 °C in order to remove the oxide layer and to form the eutectic Au-GaAs drops on the GaAs surface. After the annealing, the GaAs layers with the effective thicknesses of 500 nm (sample No. 1) and 1000 nm (sample No. 2) nm were deposited. The deposition rate of GaAs $W=1.0$ ML/s and the substrate temperature $T=585$ °C were kept constant for both the samples studied. The visualization of surface morphology was performed by applying the CamScan S4-90FE scanning electron microscope (SEM) with a field emission gun, operating in the regime of secondary electron emission. The energy of primary beam amounted to 20 keV. Cross-sectional SEM images of samples 1 and 2 are presented in Figs. 4 and 5, respectively.

IV. RESULTS AND DISCUSSION

From the analysis of SEM images of samples Nos. 1 and 2 we obtained the experimental length/diameter dependencies of NWs presented in Figs. 6 and 7. From $L(D)$ curves it is seen that the length of NWs decreases with their diameter for both the samples. For sample No. 1, the minimum diameter is about 30 nm and the maximum is about 170 nm. The

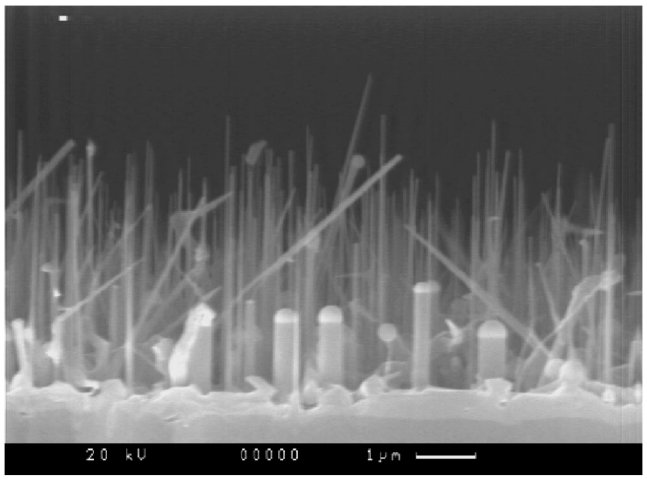

FIG. 5. SEM image of sample 2, $d_{Au}=2.5$ nm, effective thickness of GaAs=1000 nm.

length of NWs amounts to 3600 nm at $D=30$ nm and decreases to 420 nm at $D=170$ nm, the L/D ratio thus changing from 120 for the thinnest NWs down to 2.4 for the thickest ones. The maximum length of NWs is more than 7 times higher than the effective thickness of deposited GaAs. Since the thickness of Au layer for sample 2 is 2.5 times larger, the drops and resulting NWs are considerably broader—from 60 to 450 nm in diameter. The maximum length of NWs is about 4700 nm and is 4.7 times higher than the effective thickness of deposited GaAs. The L/D ratio in sample No. 2 still reaches 80 times for the thinnest NWs. The accuracy of experimental measurements and data processing is about higher than 5% for NW length and 15% for their diameter.

Theoretical $L(D)$ dependencies given by Eqs. (11) and (12) are presented in the same figures. The best fit to the experimental results for both the samples is provided at $R_c=100$ nm. This seems reasonable because the samples were grown at the same surface temperature and growth rate, so all the parameters in Eq. (10) for R_c (the unknown σ is supposed to be ~ 1) should be considered as being equal. We

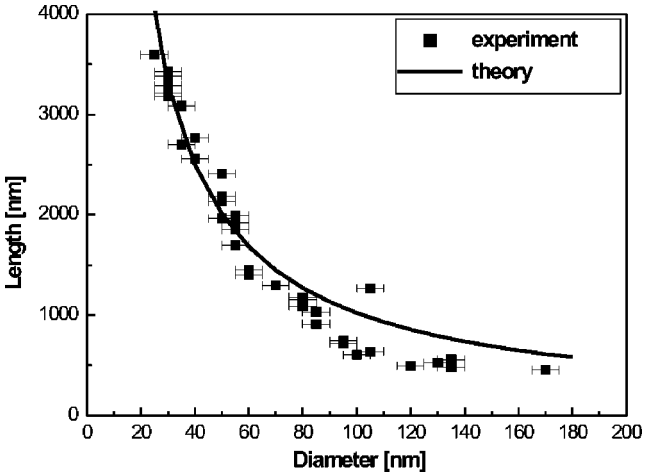

FIG. 6. Experimental and theoretical length/diameter dependencies for sample No. 1. The theoretical curve is obtained from Eqs. (11) and (12) at $H=500$ nm, $R_c=100$ nm, $\gamma=0.15$, and $\varepsilon=0.2$.

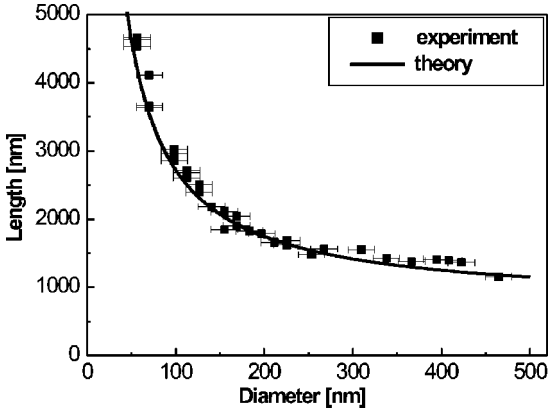

FIG. 7. Same as Fig. 6 for sample No. 2, theoretical curve obtained at $H=1000$ nm, $R_c=100$ nm, $\gamma=0.15$, and $\varepsilon=0.9$.

may therefore conclude that the MBE growth of GaAs NWs on the GaAs(111)B surface activated by Au at given growth conditions implies the domination of the DI growth for drops smaller than 100 nm. However, at the reasonable value of $\gamma=0.15$ we needed different ε to fit the two experimental curves ($\varepsilon=0.2$ for sample No. 1 and 0.9 for sample No. 2). Possible explanation of this fact is a larger perimeter of NWs in sample No. 2 per unit surface area and a higher rate of overall adatom consumption by the growing NWs in this case. Therefore, the surface growth rate in sample No. 2 is lower than in sample No. 1, and the parameter ε for sample No. 2 is larger. Also, it should be noted that neither of our experimental curves obeys the simple $1/D$ dependence of Eq. (14) within the whole range of NW lengths and diameters. This is in contrast to the recent results on the MBE grown Si NWs,[19] where the $1/D$ dependence was found to fit the experimental $L(D)$ curves for all D from 70 up to 230 nm. Therefore, while our results qualitatively agree with the results of Ref. 19 and give the decreasing $L(D)$ curves, the shape of our curves for sufficiently high NWs (>1000 nm) always contain the nonlinear terms in D.

In our previous experiments with larger drops and lower amounts of deposited GaAs (200–300 nm) we did not observe the decreasing $L(D)$ dependences and did not get the NWs with lengths several times higher than the effective thickness. In particular, in Ref. 14 the VLS-like increasing $L(D)$ dependencies were obtained that were comfortably fitted by the generalized Givargizov-Chernov theory of Ref. 17. This indicates that, depending on the MBE growth conditions and the size of initial drops, both VLS-controlled and diffusion-controlled modes of NW growth can be realized. One of the interesting effects here might be the competition between the two modes resulting in nonmonotonic $L(D)$ dependencies. Numerical study of the derived equations for the NW length/diameter dependences show the strong influence of fitting parameters R_c and ε on the resulting curves. From these two parameters only R_c can be estimated with reasonable accuracy and ε remains completely unknown. Therefore, the complete theoretical description of NWs grown by MBE should include a detailed study of all kinetic processes on the surface. The adatom diffusion to NWs may considerably reduce the surface growth rate and change the whole

picture of epitaxial growth on the nonactivated surface. This effect requires a separate study.

Finally, we have shown theoretically and experimentally that the adatom diffusion from the substrate to the top of NWs during MBE growth of GaAs NWs on the GaAs(111)B-Au surface considerably increases the length of NWs. The growth of thin NWs ($<$100 nm) is mainly controlled by the adatom diffusion and not so strongly by the adsorption on the drop surface. The length/diameter dependences of GaAs NWs exhibit the decreasing behavior typical for the DI growth. We demonstrated the possibility of growing long NWs (up to 5000 nm) with very high length/diameter ratios ($>$100) at modest amount of deposited GaAs. We have presented a kinetic model of the DI growth of NWs during MBE that explains the observed effects and shows a good qualitative correlation with the experimental results. In particular, the model explains the shape of the observed length/diameter curves.

ACKNOWLEDGMENTS

G.E.C. is grateful for the Alexander von Humboldt Foundation. The authors are grateful to the financial support from SANDIE program, different scientific programs of the Russian Academy of Sciences and RFBR Grant No. 05-02-16495.

*E mail address: v_dubr@mail.ru

[1] K. Hiruma, M. Yazawa, T. Katsuyama, K. Ogawa, K. Haraguchi, and M. Koguchi, Jpn. J. Appl. Phys., Part 1 **77**, 447 (1995).
[2] Y. Cui and C. M. Lieber. Science **91**, 851 (2000).
[3] Y. Arakawa, T. Yamauchi, and J. N. Schulman, Phys. Rev. B **43**, 4732 (1991).
[4] J.-B. Xia and K. W. Cheah, Phys. Rev. B **55**, 15 688 (1997).
[5] Y. Cui, J. L. Lauhon, M. S. Gudiksen, J. Wang, and C. M. Lieber, Appl. Phys. Lett. **78**, 2214 (2001).
[6] X. Duan, J. Wang, and C. M. Lieber, Appl. Phys. Lett. **76**, 1116 (2000).
[7] T. I. Kamins, X. Li, and R. Stanley Williams, Appl. Phys. Lett. **82**, 263 (2003).
[8] J. Westwater, D. P. Gosain, S. Tomiya, S. Usui, and H. Ruda, J. Vac. Sci. Technol. B **15**, 554 (1997).
[9] P. Finnie and Y. Homma, J. Cryst. Growth **201**, 604 (1999).
[10] B. J. Ohlsson, M. T. Björk, M. H. Magnusson, K. Deppert, and L. Samuelson, Appl. Phys. Lett. **79**, 3335 (2001).
[11] R. S. Wagner and W. C. Ellis, Appl. Phys. Lett. **4**, 89 (1964).
[12] D. N. Mcllroy, A. Alkhateeb, D. Zhang, D. E. Aston, A. C. Marcy, and M. G. Norton, J. Phys.: Condens. Matter **16**, R415 (2004).
[13] *Handbook of Crystal Growth, v.2: Bulk Crystal Growth*, edited by D. T. J. Hurle (Elsevier, North-Holland, 1994).
[14] A. A. Tonkikh, G. E. Cirlin, Yu. B. Samsonenko, I. P. Soshnikov, and V. M. Ustinov, Semiconductors **38**, 1217 (2004).
[15] E. I. Givargizov, J. Cryst. Growth **31**, 20 (1975).
[16] E. I. Givargizov and A. A. Chernov, Kristallografiya **18**, 147 (1973).
[17] V. G. Dubrovskii and N. V. Sibirev, Phys. Rev. E **70**, 031604 (2004).
[18] A. Y. Cho and J. R. Arthur, Prog. Solid State Chem. **10**, 157 (1975).
[19] L. Schubert, P. Werner, N. D. Zakharov, G. Gerth, F. M. Kolb, L. Long, U. Gösele, and T. Y. Tan, Appl. Phys. Lett. **84**, 4968 (2004).
[20] G. W. Sears, Acta Metall. **1**, 457(1953).
[21] G. W. Sears Acta Metall. **3**, 367(1955).
[22] W. Dittmar and K. Neumann, in *Growth and Perfection of Crystals*, edited by R. H. Doremus, B. W. Roberts, and D. Turnball (Wiley, New York, 1958).
[23] W. Dittmar and K. Neumann, Z. Elektrochem. **64**, 297 (1960).
[24] S. Koshiba, Y. Nakamura, M. Tsuchiya, H. Noge, H. Kano, Y. Nagamune, T. Noda, and H. Sakaki, J. Appl. Phys. **76**, 4138 (1994).
[25] S. A. Kukushkin and A. V. Osipov, Prog. Surf. Sci. **51**, 1 (1996).
[26] T. Takebe, M. Fujii, T. Yamamoto, K. Fujita, and T. Watanabe, J. Appl. Phys. **81**, 7273 (1997).